ac Dynamics of a Pinned Flux-Line Lattice

W. Henderson* and E. Y. Andrei
Department of Physics and Astronomy, Rutgers University, Piscataway, New Jersey 08855

M. J. Higgins and S. Bhattacharya
NEC Research Institute, 4 Independence Way, Princeton, New Jersey 08540

(Received 5 March 1997)

The surface impedance of $2H$-$NbSe_2$ in the mixed state was measured over the frequency range 10–3000 MHz in fields up to 2 T. A crossover between pinned and viscous flux-line dynamics is observed at a pinning frequency, ω_p. The measured ω_p is compared to that predicted by a single-particle "washboard potential" model of pinning. When the flux lattice is in an ordered state, ω_p is in good agreement with the model. However, when it is in a metastable disordered state, ω_p is nearly two orders of magnitude larger than expected, indicating the appearance of internal degrees of freedom and glassy dynamics. [S0031-9007(97)04967-3]

PACS numbers: 74.60.Ge, 74.60.Ec, 74.60.Jg

Pinning of the magnetic flux-line lattice (FLL) due to material disorder plays an important role in the transport properties of type-II superconductors [1]. When pinning prevents the FLL from moving, dc transport is nondissipative and screening of electromagnetic fields is enhanced. In the moving state, pinning can cause tears in the elastic structure of the FLL leading to plastic flow. The effects of pinning have recently been the subject of intense study, resulting in observations of phenomena such as current induced annealing [2–4], flow along weakly pinned channels [4–6], and finite response times to large current pulses [4,7]. So far, most studies of pinning have focused on transport near the dc critical current density, j_c, at which the FLL breaks loose from the pinning centers and starts moving. A complementary approach, which we present here, is to probe the local properties of the pinning potential by measuring the frequency dependence of the response to subcritical ac currents [8].

Since a flux line is essentially massless [1], the equation of motion for small oscillations in the pinned state is [9]

$$\eta \dot{u} + \kappa_p u = \Phi_0 j(t) . \tag{1}$$

where $j(t) = je^{-i\omega t}$ is the ac driving current density and u is the displacement from equilibrium. The restoring force constant κ_p is given by the curvature of the pinning potential, and the viscosity η is usually taken as $\eta = \Phi_0 H_{c2}/\rho_n$ (the Bardeen-Stephen value), with H_{c2} the upper critical field and $\Phi_0 = \frac{h}{2e}$ the flux quantum. A characteristic pinning frequency, $\omega_p = \kappa_p/\eta$, separates the low frequency regime, where pinning dominates and the response is nondissipative, from a high frequency regime of free flux motion with viscous response [9,10]. The pinning potential in periodic systems (such as charge density waves or a Wigner crystal) is usually described by the "washboard" model in which the lattice is replaced by a particle trapped in a periodic potential, $V(u) = V_0[1 - \cos(k_0 u)]$, with $k_0 = 2\pi/r_p$ determined by a characteristic length scale r_p of the pinning interaction (usually taken as the lattice spacing). For the FLL the washboard model gives $j_c = \frac{k_0 V_0}{\Phi_0}$, $\kappa_p = V_0 k_0^2$, and predicts a simple connection between ω_p and j_c,

$$\omega_p = \frac{\kappa_p}{\eta} = \frac{k_0 \rho_n}{H_{c2}} j_c . \tag{2}$$

In this Letter we report on the first measurements of the pinning frequency of the FLL in the low T_c superconductor $2H$-$NbSe_2$. The experiments employed a novel broadband technique (described below) for measuring the ac response in the mixed state in the range 10–3000 MHz. We find that ω_p exhibits a striking sensitivity to the state of the FLL: For the same field and temperature it can differ by as much as two orders of magnitude, depending on the extent of disorder in the FLL. This in turn depends on how the FLL is prepared: If the FLL is prepared by zero field cooling to $T < T_c$ and then applying a field H, it enters an ordered state for $T < T_m(H)$ and a disordered state for $T > T_m(H)$ [4]. Here $T_m(H)$ is a transition line marked by a sudden rise in j_c. However, the disordered state is always obtained when the field is applied before cooling. Below T_m the disordered state is metastable and can be annealed into the ordered state with a large current. These two states of the FLL are possible candidates for the proposed vortex glass [11] (disordered) and pinned lattice or Bragg glass (ordered) [12]. Our present results show that, in the ordered state, ω_p is in good agreement with predictions of the washboard model for the measured j_c but, in the disordered state, ω_p is much larger and the model breaks down. This breakdown of the single-particle model signals the appearance of internal degrees of freedom and glassy dynamics in the disordered FLL.

Measurements were carried out on two single-crystal samples. For sample 1 ($2.5 \times 2.5 \times 0.1$ mm) $T_c = 7.2$ K, $\Delta T_c = 80$ mK, $H_{c2}(3K) = 3.25$ T, and the residual resistance ratio, RRR = 23. This sample was grown by vapor transport from a high purity stoichiometric mixture of Nb and Se. Sample 2 ($4 \times 4 \times 0.025$ mm)

was grown by the same method from a commercial $NbSe_2$ powder containing 200 ppm of Fe impurities, resulting in $T_c = 5.85$ K, $\Delta T_c = 80$ mK, $H_{c2}(3K) = 2.0$ T, and RRR = 9. The Fe content accounts for the depressed T_c [13], but the narrow transition indicates good homogeneity. Both types of samples exhibit the phenomena reported here. We focus on sample 2 which was measured more extensively.

At finite frequencies when, due to shielding currents, the electromagnetic field penetrates only partially into the sample, the directly accessible quantity characterizing the response is the surface impedance, $Z_s = R_s - iX_s$ [14]. For example, when an rf signal propagates along a transmission line, the surface resistance R_s determines the dissipation, and the surface reactance X_s introduces a phase shift. Z_s is related to the resistivity, ρ and the penetration depth Λ, by $Z_s = (-i\mu_0\omega\rho)^{1/2} = -i\mu_0\omega\Lambda$. For a normal metal, $\Lambda = \delta_n(1 + i)/2$, with $\delta_n = (2\rho_n/\mu_0\omega)^{1/2}$ the normal state skin depth. In the mixed state, the penetration depth is determined by the response of Cooper pairs, normal fluid, and flux lines [15]:

$$\Lambda = \left(\frac{\lambda^2 + i\delta_v^2/2}{1 - 2i\lambda^2/\delta_{nf}^2}\right)^{1/2}. \tag{3}$$

Here λ is the London penetration depth, δ_{nf} is the normal fluid skin depth, $\delta_v = (2\rho_v/\mu_0\omega)^{1/2}$ is the flux-line skin depth, and ρ_v is the flux-line resistivity [16]:

$$\rho_v(\omega) = \rho_{v1}(\omega) - i\rho_{v2}(\omega) = \frac{\omega^2 - i\omega\omega_p}{\omega^2 + \omega_p^2}\,\frac{H}{H_{c2}}\,\rho_n\,. \tag{4}$$

Our results will be expressed in terms of the reduced variables, $r_s = \frac{R_s(T,H)}{R_s(T_c,0)} = \mathrm{Im}(\frac{2\Lambda}{\delta_n})$ and $x_s = \frac{X_s(T,H)}{X_s(T_c,0)} = \mathrm{Re}(\frac{2\Lambda}{\delta_n})$, which eliminate the $\omega^{1/2}$ dependence, due to the skin effect [17]. Most of our results are in a range of H, T, and ω, where the response is dominated by the flux lines. In this limit, $\Lambda = \delta_v(1 + i)/2$ and

$$r_s - ix_s = (-2i\rho_v/\rho_n)^{1/2}. \tag{5}$$

In the free flux flow limit ($\omega \gg \omega_p$), the response reduces to that of a normal metal with resistivity $\rho_n \frac{H}{H_{c2}(T)}$:

$$r_s(T,H) = x_s(T,H) = [H/H_{c2}(T)]^{1/2}, \qquad T \le T_c(H)\,. \tag{6}$$

Figure 1 shows the experimental setup [7]. The sample is mounted on a sapphire plate, which is attached to a stainless steel holder inside a vacuum can. A 50 Ω coplanar transmission line, consisting of three Cu strips (one central conductor between two ground planes) on an alumina substrate, is placed close to the sample. The sample R_s (X_s) introduces a slight change ($\le 10^{-4}$) in the magnitude (phase) of the signal propagating along the transmission line, V_{rf}. The mixer puts out a dc signal, $V_{\mathrm{IF}} \propto |V_{\mathrm{rf}}|\cos\phi$, where ϕ is the phase difference between the signals at the rf and LO ports of the mixer. The value of

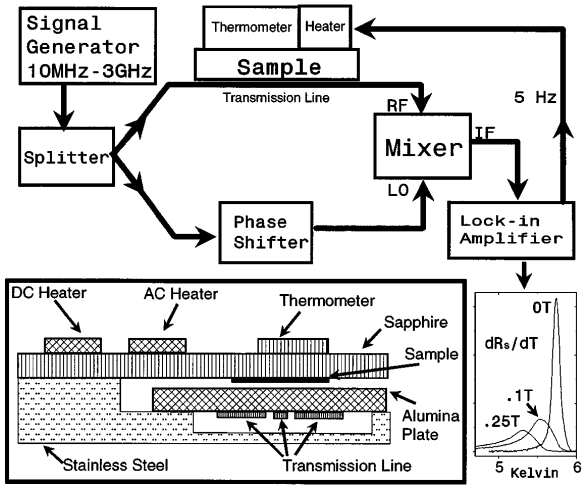

FIG. 1. Schematic view of spectrometer (upper panel) and sample holder with transmission line (lower panel).

V_{IF} is determined mainly by attenuation and phase shifts in the cables. The effect of the sample's surface impedance on V_{IF} is isolated by modulating the sample temperature at a low frequency (~5–10 Hz) with a resistive heater. This creates a small ac component in V_{IF} at the modulation frequency proportional to $\cos(\phi)\frac{dR_s}{dT} + \sin(\phi)\frac{dX_s}{dT}$, which is detected with a lock-in amplifier. By tuning ϕ to 0 or $\pi/2$, $\frac{dR_s}{dT}$ and $\frac{dX_s}{dT}$ were measured independently. The data were taken in the linear regime: the ac current in the sample was ~1 mA ($j \sim 1$ A/cm$^2 \ll j_c$) and the displacement of the flux lines (<0.1 Å at 10 MHz) was negligible compared to their spacing. H was along the c axis, and the ac current was in the a-b plane.

We first present the results in the disordered state which is prepared by cooling from above T_c to 3 K in constant H. In Fig. 2 we show the T dependence of r_s and x_s. The data were obtained by slowly ramping T as $\frac{dR_s}{dT}$ or $\frac{dX_s}{dT}$ was measured. The raw data were integrated to give $R_s^*(T) = \int_{T_0}^{T} \frac{dR_s(T')}{dT'}\,dT'$, where $T_0 = 3$ K was the lowest experimental temperature. To obtain r_s from R_s^*, two constants are needed: a scaling factor and an additive constant, $r_0 = r_s(3\ \mathrm{K})$. For $H = 0$, r_0 is assumed to be zero since we expect $R_s \simeq 0$ for $T \ll T_c$, and the scaling factor is determined by requiring $r_s(T_c, 0) = 1$. At finite H the scaling factor remains unchanged (because the coupling between the sample and transmission line is independent of H) and $r_0(H)$ is set by using the fact that $r_s(T_c, H) = 1$ (because R_s is independent of H in the normal state). The same basic procedure was used for the reactance data, but in this case $x_0 \equiv x_s(3\ \mathrm{K}, 0) = 2\lambda(3\ \mathrm{K}, 0)/\delta_n$ is always finite and x_0 was determined by fitting the data to (3), as described below.

The T dependence of r_s at 2.8 GHz is shown in Fig. 2(a). At $H = 0$, $r_s(T)$ exhibits a sharp transition and is flat below T_c, consistent with our assumption that $R_s(T \ll T_c, 0) = 0$. For $H > 0$, r_s remains nonzero

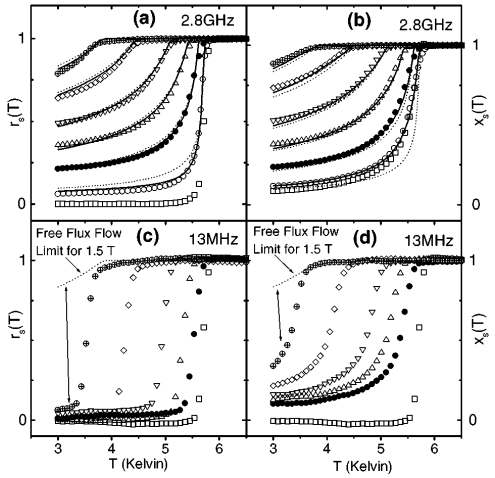

FIG. 2. The T dependence of the surface resistance and reactance at 2.8 GHz [(a) and (b)] and 1 MHz [(c) and (d)] for zero field (□), 0.02 T (○), 0.1 T (●), 0.25 T (△), 0.5 T (▽), 1 T (◇), and 1.5 T (⊗). The FLL was field cooled in all cases. The dotted lines were calculated using (6); the solid lines were calculated using (3). The double arrows show the deviation from the free flux flow case.

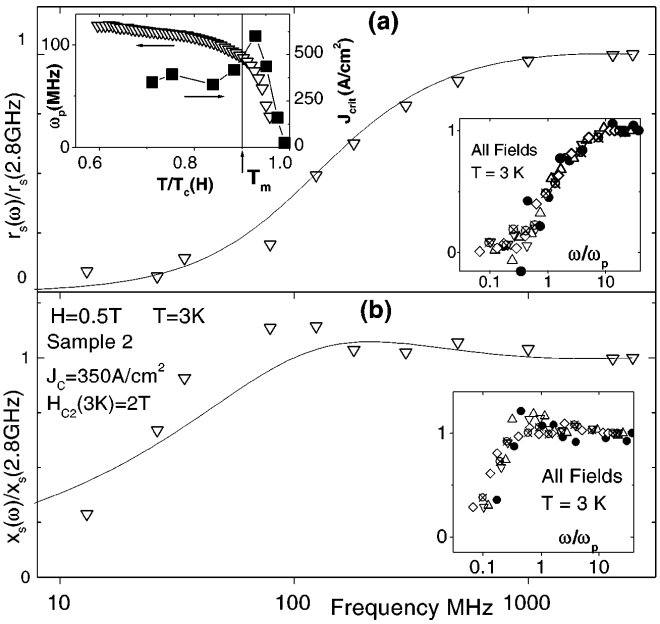

FIG. 3. The frequency dependence of R_s (a) and X_s (b) at 3 K and 0.5 T in the disordered state. Upper inset (a): temperature dependence of the pinning frequency (▽) and the critical current (■) at 0.5 T. Lower insets [(a) and (b)]: the collapse of the data for all fields. Symbols are the same as in Fig. 2.

below $T_c(H)$, indicating dissipation due to flux-line motion. The increase in r_s with H reflects the increasing flux-line density. The dotted lines, calculated in the free flux flow limit from (6), have no adjustable parameters since $H_{c2}(T)$ was obtained from dc measurements of $T_c(H)$. For $H \geq 0.1$ T this expression gives good agreement with the data, indicating that at 2.8 GHz pinning is negligible, i.e. that the pinning frequency for the disordered state $\omega_p^d \ll 2.8$ GHz. At lower H, when δ_v becomes comparable to λ, the response is no longer dominated by the FLL, and the full expression (3) must be used. Fitting the data with x_0 as an adjustable parameter (solid lines), we obtain $x_0 \sim 0.09$ at 2.8 GHz. This value was used to process the reactance data shown in Fig. 2(b). The r_s and x_s data for $H < 0.1$ T over the entire temperature range could be fitted with this single parameter, which indicates that (3) correctly describes the interplay between the response of the flux lines and the Cooper pairs. Since $x_0 = \frac{2\lambda(3\text{ K},0)}{\delta_n}$ and δ_n depends only on ρ_n, which was measured, the value of x_0 can be used to determine λ. From the data at several frequencies in the GHz range, we estimate $\lambda \sim 1200-1400$ Å in sample 2 and $\sim 1000-1200$ Å in sample 1. Previous estimates are scattered over the range 700–2500 Å [18].

In Figs. 2(c) and 2(d) we show the results at 13 MHz. In this case, both r_s and x_s drop well below the free flux flow values (dotted lines), indicating that $\omega_p^d > 13$ MHz. The frequency dependence of the response over the entire range, Fig. 3, exhibits a crossover from pinned to viscous behavior. Fitting the data to (5), with ρ_v given by (4), gives $\omega_p^d = 125$ MHz for $H = 0.5$ T and $T = 3$ K. The lower insets in Fig. 3 show that the data for all H collapse when plotted as a function of $\omega/\omega_p^d(T,H)$. This universal behavior shows that the frequency dependence of the response of the FLL is completely characterized by one parameter ω_p^d as expected from (1).

We now turn to the response in the ordered state. In this state, if the FLL is heated above T_m, it undergoes an order-to-disorder transition that is irreversible in temperature [4]. Thus $\frac{dR_s}{dT}$ and $\frac{dX_s}{dT}$ cannot be obtained over the entire temperature range and the additive constants needed to determine the absolute values of r_s and x_s cannot be calculated. But from the relative changes, $\Delta r_s(T)$ and $\Delta x_s(T)$, which can be measured directly, we find that for frequencies in the GHz range the results are identical to those obtained for the disordered FLL, whereas in the MHz range they differ significantly. In Fig. 4(a) we plot $\Delta r_s(T)$ at 13 MHz in both states. The data in the disordered state is essentially constant in T, consistent with the high value of ω_p^d. However, in the ordered state the results are consistent with free flux flow [the slope in $\Delta r_s(T)$ is close to that at 2.8 GHz] indicating that ω_p^0, the pinning frequency of the ordered FLL, is in the MHz range or lower. Below 1 MHz, δ_v is much greater than the sample thickness, and therefore ρ_v can be accessed directly with a standard four-lead technique. The data for ρ_{v1} and ρ_{v2} in both states are shown in Fig. 4(b). They were taken on a sample which was from the same batch as sample 2 and had nearly identical parameters. A background signal, due to pickup, was determined from zero field measurements at $T \ll T_c$ and subtracted from the data. In the disordered state both ρ_{v1} and ρ_{v2} are

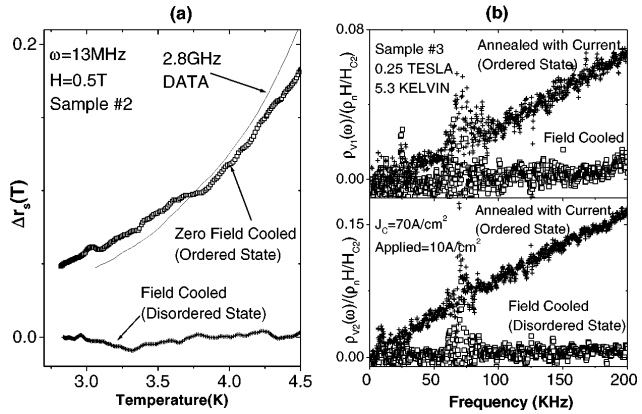

FIG. 4. Comparisons of the ac response for the field-cooled state and the ordered state below T_m. (a) $\Delta r_s(T)$ at 13 MHz. (b) The frequency dependence of the complex resistivity. The noise near 75 KHz is instrumental.

vanishingly small over the entire frequency range, indicating that $\omega_p^d \gg 200$ kHz, in accord with the above results. By contrast, ρ_{v1} and ρ_{v2} are finite in the ordered state and their frequency dependence gives $\omega_p^0 \sim 1$ MHz.

To interpret the results we use the washboard model (2) to compare the measured ω_p and j_c. For the ordered state data shown in Fig. 4(b), $j_c = 70$ A/cm^2 and the washboard model gives $\omega_p^0 = 1.4$ MHz, in rough agreement with the data. In the disordered state there is a large discrepancy between the magnitude of the measured ω_p and the predictions of the model: For example, at 3 K and 0.5 T, where $j_c = 350$ A/cm^2, the model gives $\omega_p = 2.6$ MHz which is 45 times lower than the measured value. This discrepancy is similar everywhere in the H-T plane, except above $T_m(H)$, where it is smaller. Moreover, ω_p^d and j_c exhibit a qualitatively different temperature dependence [upper inset of Fig. 3(a)]. This is especially pronounced near T_m, where j_c increases with T while ω_p decreases. Thus, the washboard model, which successfully describes the ordered state, fails for the metastable disordered state. The reason for this failure is inherent in the single-particle treatment of the problem, in which j_c is the current to drive the entire FLL out of the pinning potential. However, if the flux lattice reorders prior to becoming completely depinned (i.e., plastic flow occurs during the depinning process), j_c can actually occur earlier: at a current at which the FLL becomes unstable to the creation of channels of mobile flux lines. Evidence for rearrangement and channel growth was previously observed with dc [4,5] and pulsed current measurements [4,7], as well as in computer simulations [6]. However, the ac measurements are not affected because the rearrangements cannot occur at the low driving currents and the short time scales of these measurements.

The measurements described here have shown that the ordered FLL behaves as an elastic medium, whereas the disordered FLL exhibits metastability and plastic flow associated with internal degrees of freedom. The same behavior was also observed in sample 1 (the discrepancy between j_c and ω_p was actually larger in this sample), even though little evidence of metastability and plastic dynamics could be detected in dc measurements. (Metastability was also clearly seen in pulsed current measurements on this sample.) This suggests that, although metastability effects are not typically seen in dc transport, they may, in fact, be common in flux lattices.

We thank N. Andrei, D. Huse, and R. Walstedt for useful comments; M. McElfresh and P. McDowel for sample characterization; S. Max for technical help. This paper was supported by NSF-DMR-9401561 and 97-05389.

*Current address: Department of Physics, University of California, Los Angeles, California 90024-1547.

[1] G. Blatter *et al.*, Rev. Mod. Phys. **66**, 1125 (1994).
[2] R. Wördenweber, P. H. Kes, and C. C. Tsuei, Phys. Rev. B **33**, 3172 (1986).
[3] U. Yaron *et al.*, Phys. Rev. Lett. **73**, 2748 (1994).
[4] W. Henderson, E. Y. Andrei, M. J. Higgins, and S. Bhattacharya, Phys. Rev. Lett. **77**, 2077 (1996).
[5] S. Bhattacharya and M. Higgins, Phys. Rev B **52**, 64 (1995); M. Hellerqvist *et al.*, Phys. Rev. Lett. **76**, 4022 (1996).
[6] H. J. Jensen, A. Brass, and A. J. Berlinsky, Phys. Rev. Lett. **60**, 1676 (1988); N. Grønbech-Jensen, A. R. Bishop, and D. Domínguez, Phys. Rev. Lett. **76**, 2985 (1996); C. Reichhardt *et al.*, Phys. Rev. B **53**, R8898 (1996).
[7] W. Henderson, Ph.D. thesis, Rutgers University, 1996.
[8] This approach was used in studies of pinning in the Wigner crystal [E. Y. Andrei *et al.*, Phys. Rev. Lett. **60**, 2765 (1988); F. I. B. Williams *et al.*, Phys. Rev. Lett. **66**, 3285 (1991)].
[9] J. Gittleman and B. Rosenblum, Phys. Rev. Lett. **16**, 734 (1966).
[10] A crossover as a function of H was observed in J. Owliaei, S. Sridhar, and J. Talvacchio, Phys. Rev. Lett. **69**, 3366 (1992).
[11] M. J. P. Gingras and D. A. Huse, Phys. Rev. B **53**, 15 193 (1996).
[12] T. Giamarchi and P. Le Doussal, Phys. Rev. B **52**, 1242 (1995).
[13] K. Noto *et al.*, Physica (Amsterdam) **99B**, 204 (1980); J. J. Hauser *et al.*, Phys. Rev. B **8**, 1038 (1973).
[14] C. Kittel, *Quantum Theory of Solids* (Wiley, New York, 1987).
[15] M. Coffey and J. Clem, Phys. Rev. Lett. **67**, 386 (1991); Phys. Rev. B **46**, 11 757 (1992); E. Brandt, Phys. Rev. Lett. **67**, 2219 (1991); C. J. van der Beek, V. B. Geshkenbein, and V. M. Vinokur, Phys. Rev. B **48**, 3393 (1993).
[16] ρ_v is given by Ohm's law $\rho = E/j$, with $E = \dot{u} \times H$ determined by solving Eq. (1) for the flux-line velocity $\dot{u}$.
[17] For all of the data, δ_n is independent of H and T, as determined from measurements of ρ_n.
[18] P. de Trey *et al.*, J. Low Temp. Phys. **11**, 421 1973; R. E. Schwall *et al.*, J. Low Temp. Phys. **22**, 557 (1976); K. Takita *et al.*, J. Low Temp. Phys. **58**, 127 (1985); L. P. Le *et al.*, Physica (Amsterdam) **185C-189C**, 2715 (1991).